

Dynamically Solving the μ/B_μ Problem in Gauge-mediated Supersymmetry Breaking

Tao Liu^{a,1} and Carlos E.M. Wagner^{a,b,c,2}

^a Enrico Fermi Institute and ^b Kavli Institute for Cosmological Physics,
University of Chicago, 5640 S. Ellis Ave., Chicago, IL 60637

^c HEP Division, Argonne National Laboratory, 9700 Cass Ave., Argonne, IL 60439

Abstract

We provide a simple solution to the μ/B_μ problem in the gauge-mediated Next-to-Minimal Supersymmetric Standard Model. In this model the messenger sector contains one pair of $3 + \bar{3}$ and one pair of $2 + \bar{2}$ messengers. These two messenger pairs couple to different gauge singlets in the hidden sector in which supersymmetry (SUSY) is broken. Such a gauge-mediation structure can naturally arise in many backgrounds. Because of the two effective SUSY breaking scales $\frac{\langle F_i \rangle}{\langle M_i \rangle}$ in the messenger sector, the renormalization group evolutions of the soft SUSY breaking parameters can be properly modified, leading to a negative enough singlet soft mass square $m_N^2(\Lambda_{EW})$ and hence reasonable μ/B_μ values. In most of the perturbative (up to the GUT scale) parameter region, as a result, the electroweak scale is stabilized and phenomenologically interesting mass spectra of particles and superparticles are obtained. In addition, this model favors large values of $\tan \beta$: $5 \sim 50$ and a heavy scalar spectrum. With the relatively large $\tan \beta$, the light $U(1)_R$ pseudoscalar (mainly appearing in the low-scale gauge-mediated SUSY breaking models) becomes extremely singlet-like, and is no longer a problem in this model. These features apply to all cases of low-, intermediate- and high-scale gauge-mediated SUSY breaking.

¹Email: taoliu@theory.uchicago.edu

²Email: cwagner@hep.anl.gov

1 Introduction

The Standard Model (SM) provides an excellent description of all particle physics interactions, excluding gravity. The excellent agreement of the SM predictions with the measured precision electroweak (EW) physics observables would be recovered in any extension of the SM in which the new physics decouples fast from physics at the weak scale. Supersymmetry (SUSY) is an example of such an extension. Supersymmetric particles receive contribution to their masses through gauge invariant operators which are independent of the Higgs mechanism, and their effects decouple fast as these masses are increased. Since these contributions to the slepton and squark masses are not necessarily aligned in flavor space with the lepton and quark masses, new flavor violating contributions become significant, leading to a potential conflict with flavor physics observables.

In gauge mediated SUSY breaking models, SUSY breaking masses are flavor independent at the messenger scale, leading to flavor violating effects that are still controlled by the Cabbibo-Kobayashi-Maskawa (CKM) matrix elements, enabling the existence of superparticles with EW scale masses. Problems remain in the Higgs sector, however, related to the origin and natural relation between the Higgsino mass parameter μ and the Higgs mixing mass term B_μ .

In the minimal supersymmetric standard model(MSSM), we need a term of the form

$$\Delta\mathcal{L} = \int d^2\theta \mu \mathbf{H}_d \mathbf{H}_u + h.c. \quad (1)$$

to give the Higgsinos a mass. If $\mu \gg \Lambda_{EW}$, the Higgs scalars in the chiral superfields obtain a large mass term in the potential and the EW symmetry may not be broken. If $\mu \ll \Lambda_{EW}$, the lightest chargino mass is lighter than m_W^2/M_2 with M_2 being the soft mass of bino and winos, and the experimental bounds can not be satisfied. Therefore we must have

$$\mu \sim \Lambda_{EW}. \quad (2)$$

However, it is hard to understand why the μ parameter is of this scale instead of the more fundamental Planck scale M_P , considering that it is not related in any direct way to the SUSY breaking sector of the MSSM. Introducing a dynamical mechanism may help solve this so-called μ problem, but generally at the price of introducing some new problems, e.g., μ/B_μ problem. The μ/B_μ problem is related to the origin of the scalar soft SUSY breaking Higgs mixing mass term,

$$\Delta V = B_\mu H_d H_u + h.c. \quad (3)$$

To stabilize the EW scale M_{EW} , it is necessary to have

$$B_\mu \sim \Lambda_{EW}^2 \sim \mu^2. \quad (4)$$

In the context of a dynamical generation of μ , however, it is difficult to generate a B_μ satisfying this relation. This is particularly true for the case of low-scale gauge-mediated SUSY breaking.

So far, there are three main mechanisms to solve the μ/B_μ problem. The first one is the Giudice-Masiero mechanism which is the first proposed to solve this problem in the context of gravity-mediated SUSY breaking [1]. Its basic idea is to assume an exact Peccei-Quinn symmetry, forbidding the μ term in the supersymmetric limit, and then generate it and B_μ dynamically according to the SUSY breaking effects of the same order. Explicitly, the authors of Ref. [1] introduce one set of higher-dimensional operators in the Kahler potential

$$\Delta\mathcal{L} = \int d^4\theta \mathbf{H}_d \mathbf{H}_u \left(\frac{c_1}{M_P} \mathbf{X}^\dagger + \frac{c_2}{M_P^2} \mathbf{X}^\dagger \mathbf{X} \right) + h.c. \quad (5)$$

here \mathbf{X} is the SUSY breaking chiral spurion. Once the SUSY is broken, the effective μ and B_μ parameters are generated as

$$\mu = \frac{c_1 \langle F_X \rangle}{M_P}, \quad B_\mu = \frac{c_2 \langle F_X \rangle^2}{M_P^2}. \quad (6)$$

Since $\frac{\langle F_X \rangle}{M_P}$ denotes the natural scale of the soft terms in the gravity-mediation case, the correct relationship

$$\frac{B_\mu}{\mu} \sim \frac{c_2 \langle F_X \rangle}{c_1 M_P} \sim \text{TeV} \quad (7)$$

arises if $c_1 \sim c_2 \sim \mathcal{O}(1)$. But this idea is hard to be translated to the gauge-mediation case. In the effective theory of gauge-mediation, the μ and B_μ operators (similar to those in Eq.(5)) are generally induced at the same loop-level. Unlike the gravity-mediation case, the effective SUSY breaking scale $\frac{\langle F_X \rangle}{\Lambda_M}$ is no longer the natural scale of the soft terms, which necessarily leads to a modified relationship between μ and B_μ

$$\frac{B_\mu}{\mu} \sim \frac{c_2 \langle F_X \rangle}{c_1 \Lambda_M} \sim \frac{\langle F_X \rangle}{\Lambda_M} \sim 100 \text{TeV}. \quad (8)$$

Here Λ_M denotes the messenger scale (unlike the gravity-mediation, c_1 and c_2 now represent the product of coupling constants and possible loop factors). Recently, it was noticed [2] that the B_μ operator in Eq.(5) is not protected by non-renormalization theorems of the hidden sector because $\mathbf{X}^\dagger \mathbf{X}$ is not a holomorphic or anti-holomorphic operator of the hidden sector. The strong dynamics in the hidden sector therefore can efficiently suppress c_2 with respect to c_1 , in the renormalization group(RG) evolution above the SUSY breaking scale $\sqrt{\langle F_X \rangle}$. However, due to the same effect, the characteristic mass spectrum of gauge mediation in the squark and slepton sectors is ruined in this model. It turns out that the physically allowed parameter region for this model is rather small [3].

A second one is the dynamical relaxation mechanism [4]. Its basic idea is to generate μ and B_μ according to the SUSY breaking effects of different orders. Explicitly, one can forbid the appearance of non-holomorphic operators and hence a B_μ operator in the effective action

of one-loop level. Then the operators from the higher-order corrections can be responsible of generating B_μ of the correct size. Such an one-loop effective action has the general form [5]

$$\Delta\mathcal{L} = \int d^4\theta \mathbf{H}_d \mathbf{H}_u [f(\mathbf{X}) + g(\mathbf{X}^\dagger) + D^2 h(\mathbf{X}, \mathbf{X}^\dagger)] + h.c. \quad (9)$$

with D_α being the supersymmetric covariant derivative and f, g, h being generic functions of SUSY breaking chiral spurion \mathbf{X} . These one-loop effective operators can be induced by a proper construction of the superpotential in the messenger sector. The effective μ term then arise according to the second term [5] or the third one [4] which are characterized by a divergent logarithmic form of $\mathbf{X}^\dagger \mathbf{X}$ in this mechanism. As for the B_μ term, it will be generated at a higher order in perturbation theory. This mechanism is similar to that of the soft mass generation of squarks and sleptons. But, compared to the naturalness of the latter due to the absence of couplings between the squarks, sleptons and the messenger sector at tree level, the structure of the required superpotential for the former is typically non-generic. Actually, a new dimensional parameter is introduced again in the superpotential of the messenger sector [4, 5].

The third one is the light singlet mechanism which is also the focus of this paper. In this scenario, the μ term is forbidden by some discrete symmetries (e.g., in the Next-to-Minimal Supersymmetric Standard Model (NMSSM) and the nearly-Minimal Supersymmetric Standard Model (nMSSM)) or by some additional Abelian gauge symmetry (e.g., in the $U(1)'$ -extended Minimal Supersymmetric Standard Model (UMSSM) [11]). With the introduction of a singlet chiral superfield \mathbf{N} in the observable sector which has the coupling

$$\Delta\mathcal{L} = \int d^2\theta \lambda \mathbf{N} \mathbf{H}_d \mathbf{H}_u + h.c. \quad (10)$$

the effective μ and B_μ parameters arise as

$$\mu \equiv \lambda v_N, \quad B_\mu \sim \lambda \langle F_N \rangle, \quad (11)$$

after the SUSY is broken. So, as long as the scalar N and its auxiliary field F_N are stabilized at the soft SUSY breaking scale or EW scale, a correct relationship

$$\frac{B_\mu}{\mu} \sim \frac{\langle F_N \rangle}{v_N} \sim 10^2 - 10^3 \text{GeV}. \quad (12)$$

can be achieved. But this mechanism faces serious problems: (1) to generate a proper v_N , a negative enough soft mass square $m_N^2(\Lambda_{EW})$ is required, which turns out to be a rather difficult mission, persisting for any messenger scale [6, 7]; (2) both the trilinear soft parameters $|A_\lambda(\Lambda_{EW})|$ and $|A_\kappa(\Lambda_{EW})|$ are generically small, compared to Λ_{EW} (this is due to the fact that they are highly suppressed at the messenger scale while their RG evolutions down to the EW scale are mediated by small beta functions.). Since they are the only sources explicitly breaking the global $U(1)_R$ symmetry, their smallness necessarily leads to a light pseudoscalar which, unless is mainly a singlet, is ruled out by the current LEP bound [6]. One

way to circumvent these difficulties is to make the \mathbf{N} field couple to the messengers [8] (also see [9]), or to extra light freedom degrees [6, 11]. Then a modified boundary value (at the messenger scale) or beta function of m_N^2 may help solve this problem. But, it was realized recently that the experimental bounds on the Higgs mass can add severe constraints on the former class of models [10]. As for the latter, it is viable, except that the couplings generally need to be strong $\sim \mathcal{O}(1)$ if only small number of the light freedom degrees exist [11]. In this paper, however, we will show that the problems in the light singlet mechanism are just some misguided images. In the context of a more general gauge-mediated NMSSM where the (minimal) messenger pairs $3 + \bar{3}$ and $2 + \bar{2}$ couple to different SUSY breaking chiral spurions in the hidden sector, there is no difficulty in generating a negative enough $m_N^2(\Lambda_{EW})$ in most of the perturbative (up to GUT scale) $\lambda - \kappa$ parameter region. The EW scale is then stabilized, and phenomenologically interesting mass spectra of particles and superparticles are also obtained. As a general feature, squarks and sleptons become heavy, while there are light charginos and neutralinos, which are mostly an admixture of Higgsinos and singlinos. Such an interesting gauge-mediation structure can effectively arise in many general backgrounds.

In addition, there is no light $U(1)_R$ pseudoscalar problem in our model. For the intermediate- and high-scale gauge mediations, large $|A_\lambda(\Lambda_{EW})|$ comparable with Λ_{EW} are typical, so the lightest Higgs pseudoscalar actually are not light. For the low-scale case, even though $|A_\lambda(\Lambda_{EW})|$ and $|A_\kappa(\Lambda_{EW})|$ are not always large, the lightest Higgs pseudoscalar is extremely singlet-like due to large $\tan\beta$ values, escaping the experimental constraints again. The light singlet mechanism therefore is naturally implemented, without introducing any complicated or special elements in the messenger sector. Our idea is proposed in section 2, and followed are the numerical results in section 3. The last section is our discussions and conclusions. Since different energy scales are involved for the parameters in this paper, we will specify them unless they can be understood according to the context.

2 A Simple Model to Solve $\mu/B\mu$ Problem

2.1 The NMSSM

As the simplest extension of the MSSM, the NMSSM has a superpotential for the Higgs superfields

$$\mathbf{W} = \lambda \mathbf{N} \mathbf{H}_d \mathbf{H}_u - \frac{1}{3} \kappa \mathbf{N}^3, \quad (13)$$

where the μ term in the MSSM has been forbidden by a Z_3 discrete symmetry. The cubic term of \mathbf{N} in the superpotential explicitly breaks the Peccei-Quinn symmetry

$$\mathbf{N} \rightarrow \mathbf{N} e^{i\alpha}, \mathbf{H}_d \mathbf{H}_u \rightarrow \mathbf{H}_d \mathbf{H}_u e^{-i\alpha}. \quad (14)$$

In the absence of the singlet cubic term the EW symmetry breaking would spontaneously break the Peccei-Quinn symmetry as well, and hence lead to a dangerous Peccei-Quinn Goldstone boson.

It is not hard to write down the tree-level neutral Higgs potential in the NMSSM, which consists of F -terms, D -terms, and soft SUSY-breaking terms

$$\begin{aligned}
V_0 &= V_F + V_D + V_{soft}, \\
V_F &= |\lambda H_d H_u - k N^2|^2 + \lambda^2 |N|^2 (|H_d|^2 + |H_u|^2), \\
V_D &= \frac{g_Y^2 + g_2^2}{8} (|H_d|^2 - |H_u|^2)^2, \\
V_{soft} &= m_{H_d}^2 |H_d|^2 + m_{H_u}^2 |H_u|^2 + m_N^2 |N|^2 \\
&\quad - (\lambda A_\lambda H_d H_u N + h.c.) - \left(\frac{\kappa}{3} A_\kappa N^3 + h.c. \right). \tag{15}
\end{aligned}$$

Here H_d , H_u and N denote the neutral Higgs bosons corresponding to \mathbf{H}_d , \mathbf{H}_u and \mathbf{N} , respectively.

The one-loop effective Higgs potential is formally given by

$$\Delta V = \frac{1}{64\pi^2} \text{STr} \mathcal{M}^4(H_i) \left(\ln \frac{\mathcal{M}^2(H_i)}{\Lambda_{\overline{\text{MS}}}^2} - \frac{3}{2} \right) \tag{16}$$

Here $\mathcal{M}^2(H_i)$ is a field-dependent mass-squared matrix, and $\Lambda_{\overline{\text{MS}}}$ is the $\overline{\text{MS}}$ renormalization scale at which all RG evolved parameters are fixed. Since ΔV may bring significant radiative corrections to some of the Higgs boson masses, we will include it into our analysis. Two-loop corrections to the Higgs potential will not be included, but we will comment on their possible effects at the end of this article.

Note, even though the one-loop effective Higgs potential brings an explicit dependence on $\Lambda_{\overline{\text{MS}}}$, all observables are independent of it. The mass matrix \mathcal{M}^2 depends on the fields H_i through their couplings to various other particles. Since it is the strength of these couplings, instead of the absolute values of the masses, that measures the one-loop corrections to the minimization conditions and to the Higgs mass matrix, the most important one-loop corrections come from the field-dependent masses of top quark sector and bottom quark sector (for large $\tan\beta$ case). In this paper, we will only consider their contributions to the one-loop effective Higgs potential. Explicitly, they are given by

$$\begin{aligned}
\Delta V &= \frac{3}{32\pi^2} \left[m_{\tilde{t}_1}^4(H_i) \left(\ln \frac{m_{\tilde{t}_1}^2(H_i)}{\Lambda_{\overline{\text{MS}}}^2} - \frac{3}{2} \right) + m_{\tilde{t}_2}^4(H_i) \left(\ln \frac{m_{\tilde{t}_2}^2(H_i)}{\Lambda_{\overline{\text{MS}}}^2} - \frac{3}{2} \right) \right. \\
&\quad \left. - 2m_t^4(H_i) \left(\ln \frac{m_t^2(H_i)}{\Lambda_{\overline{\text{MS}}}^2} - \frac{3}{2} \right) \right] \\
&\quad + \frac{3}{32\pi^2} \left[m_{\tilde{b}_1}^4(H_i) \left(\ln \frac{m_{\tilde{b}_1}^2(H_i)}{\Lambda_{\overline{\text{MS}}}^2} - \frac{3}{2} \right) + m_{\tilde{b}_2}^4(H_i) \left(\ln \frac{m_{\tilde{b}_2}^2(H_i)}{\Lambda_{\overline{\text{MS}}}^2} - \frac{3}{2} \right) \right. \\
&\quad \left. - 2m_b^4(H_i) \left(\ln \frac{m_b^2(H_i)}{\Lambda_{\overline{\text{MS}}}^2} - \frac{3}{2} \right) \right]. \tag{17}
\end{aligned}$$

2.2 The Model

The NMSSM provides the simplest or most direct realization of the light singlet mechanism to solve the μ/B_μ problem in gauge-mediated SUSY breaking models, where the μ/B_μ parameters are effectively generated as

$$\begin{aligned}\mu &\equiv \lambda v_N, \\ B_\mu &\equiv \lambda \langle F_N \rangle + A_\lambda \mu,\end{aligned}\tag{18}$$

here

$$\begin{aligned}v_N &= \langle N \rangle \\ \langle F_N \rangle &= \frac{\kappa}{\lambda^2} \mu^2 - \frac{\lambda v^2}{2} \sin 2\beta\end{aligned}\tag{19}$$

with $v^2 = v_d^2 + v_u^2$. But it is also confronted by the common problems of all models of the light singlet mechanism. Let us rephrase these problems in the framework of the NMSSM. Consider the minimization conditions of the tree-level Higgs potential in the NMSSM [7]

$$\mu^2 = \lambda^2 v_N^2 = -\frac{M_Z^2}{2} + \frac{m_{H_d}^2 - m_{H_u}^2 \tan^2 \beta}{\tan^2 \beta - 1},\tag{20}$$

$$B_\mu = A_\lambda \lambda v_N - \lambda(\lambda v_d v_u - \kappa v_N^2) = (m_{H_d}^2 + m_{H_u}^2 + 2\lambda^2 v_N^2) \frac{\sin 2\beta}{2},\tag{21}$$

$$2\kappa^2 v_N^2 = \lambda v^2 (\kappa \sin 2\beta - \lambda) - m_N^2 + A_\lambda \lambda v^2 \frac{\sin 2\beta}{2v_N} + \kappa A_\kappa v_N.\tag{22}$$

For the minimal gauge mediation, where the messenger sector is

$$W = \lambda \mathbf{S} \bar{\mathbf{q}} \mathbf{q} + \gamma \mathbf{S} \bar{\mathbf{l}} \mathbf{l}\tag{23}$$

with $\mathbf{S} = S + \theta^2 F_S$ being the SUSY breaking spurion field and $(\mathbf{q} + \mathbf{l}) + (\bar{\mathbf{q}} + \bar{\mathbf{l}})$ being $(3+2) + (\bar{3} + \bar{2})$ messenger pairs. The lower mass bounds of sleptons or gluinos give a lower bound on the effective SUSY breaking scale

$$\Lambda_S = \frac{\langle F_S \rangle}{\langle S \rangle}\tag{24}$$

according to their RG evolutions. This lower bound immediately implies another lower bound on the beta function of $m_{H_u}^2$ (because of its positivity), and then leads to $m_{H_u}^2(\Lambda_{EW}) \lesssim -(200\text{GeV})^2$ [7]. According to Eq.(20), this is translated into a stringent bound on the effective μ parameter or v_N for mildly large $\tan \beta$ [7]

$$|\mu| \gtrsim 200\text{GeV}.\tag{25}$$

On the other hand, due to the third minimization condition Eq.(22) a very negative $m_N^2(\Lambda_{EW})$ or very large $A_\lambda(\Lambda_{EW})$ and $A_\kappa(\Lambda_{EW})$ are necessary in order to generate a large v_N or μ for

$\lambda, \kappa \sim \mathcal{O}(1)$. This is difficult to achieve because (see the related RG equations summarized in Appendix A):

(1) For m_N^2 , as the RG evolution runs down, its beta function becomes small quickly due to the negative contribution from $m_{H_u}^2$;

(2) For A_λ and A_κ , their values at the messenger scale are highly suppressed due to their high-loop level origin and, at the same time, their beta functions are not negative enough. In addition, because A_λ and A_κ are the only sources explicitly breaking the global $U(1)_R$ symmetry in the Higgs potential, their smallness necessarily leads to an almost massless pseudoscalar which is ruled out by the current LEP bound [6].

As a result, the μ/B_μ problem is not solved in the NMSSM within the minimal gauge mediation scenario [7].

In this paper, we present a new way to solve the μ/B_μ problem within the NMSSM with gauge-mediated SUSY breaking. Actually, we only take a simple modification to the superpotential, Eq.(23), assuming the new one to be

$$W = \lambda \mathbf{S}_q \bar{\mathbf{q}} \mathbf{q} + \gamma \mathbf{S}_l \bar{\mathbf{l}}, \quad (26)$$

here $\mathbf{S}_q = S_q + \theta^2 F_q$ and $\mathbf{S}_l = S_l + \theta^2 F_l$ are two SUSY breaking chiral spurions. In the following, we will use Λ_q and Λ_l to denote the effective SUSY breaking scales, *i.e.*,

$$\Lambda_q = \frac{\langle F_q \rangle}{\langle S_q \rangle}, \quad \Lambda_l = \frac{\langle F_l \rangle}{\langle S_l \rangle}. \quad (27)$$

As explained above, the difficulty in generating a very negative $m_N^2(\Lambda_{EW})$ is from the fact that the RG evolutions of $m_{H_u}^2$ and m_N^2 are strongly coupled to each other. The parameter $m_{H_u}^2$ has a large, positive beta function, so it becomes negative quickly as the RG evolutions run down. The negative $m_{H_u}^2$ leads to a negative contribution to the beta function of m_N^2 , therefore, preventing the appearance of a large, negative $m_N^2(\Lambda_{EW})$. However, the story can be dramatically changed after the introduction of a new parameter $\eta = \Lambda_l/\Lambda_q$. In the minimal gauge mediation limit, we have $\eta = 1$. As it is increased, the beta function of m_N^2 is effectively enlarged according to the dominant terms $4\lambda^2(m_{H_d}^2 + m_{H_u}^2)$, while the beta function of $m_{H_u}^2$ is effectively diminished according to the terms $-(2g_Y^2 M_1^2 + 6g_2^2 M_2^2)$ (even though some other terms may have positive contributions to this beta function.). Due to these effects, the velocity for m_N^2 to evolve to a negative value is increased, but that for $m_{H_u}^2$ is slowed down. It becomes possible now to get a large, negative $m_N^2(\Lambda_{EW})$, even if only a mild increase is made for η . In contrast to the ‘‘minimal gauge mediation’’, we will refer to this mechanism as ‘‘general gauge mediation’’ in the following.

With the superpotential of the messenger sector modified, the soft SUSY breaking masses are also different from those generated in the minimal gauge mediation case. These new soft masses at the messenger scale are found to be (see, for instance, Ref. [12])

$$M_3 = \frac{\alpha_3}{4\pi} \Lambda_q \quad M_2 = \frac{\alpha_2}{4\pi} \Lambda_l \quad M_1 = \frac{\alpha_1}{4\pi} \left[\frac{2}{5} \Lambda_q + \frac{3}{5} \Lambda_l \right] \quad (28)$$

for gauginos, and

$$m_\phi^2 = 2 \left[C_3^\phi \left(\frac{\alpha_3}{4\pi} \right)^2 \Lambda_q^2 + C_2^\phi \left(\frac{\alpha_2}{4\pi} \right)^2 \Lambda_l^2 + C_1^\phi \left(\frac{\alpha_1}{4\pi} \right)^2 \left(\frac{2}{5} \Lambda_q^2 + \frac{3}{5} \Lambda_l^2 \right) \right], \quad (29)$$

for squarks, sleptons and neutral Higgs bosons. C_3^ϕ , C_2^ϕ and $C_1^\phi = \frac{3}{5} Y_\phi^2$ are quadratic Casimir operators of the scalar ϕ . It is easy to check that, with $\Lambda_q = \Lambda_l$, Eq.(28) and Eq.(29) reduce to the results in the minimal gauge mediation case.

The superpotential of the general gauge mediation Eq (26) can naturally arise in many backgrounds. For example, in the case where the messenger pairs $3 + \bar{3}$ and $2 + \bar{2}$ are coupled to several SUSY breaking chiral spurions $\mathbf{S}_i = S_i + \theta^2 F_i$ (e.g., see [13])

$$W = \lambda_i \mathbf{S}_i \bar{\mathbf{q}} \mathbf{q} + \gamma_i \mathbf{S}_i \bar{\mathbf{l}} \mathbf{l}, \quad (30)$$

we can assume

$$\mathbf{S}_q = \lambda_i \mathbf{S}_i, \quad \mathbf{S}_l = \gamma_i \mathbf{S}_i. \quad (31)$$

Λ_q and Λ_l then effectively arise as

$$\Lambda_q = \frac{\lambda_i \langle F_i \rangle}{\lambda_j \langle S_j \rangle}, \quad \Lambda_l = \frac{\gamma_i \langle F_i \rangle}{\gamma_j \langle S_j \rangle}. \quad (32)$$

Here the sums over the index "i" and "j" are implicitly assumed.

At last, it is necessary to point out that, with the one-loop corrections to the Higgs potential included, the constraint on the effective μ parameter given by (25) can be relaxed to some extent. As an illustration, let us consider the minimization conditions with the corrections from the stops \tilde{t}_1 and \tilde{t}_2 included

$$\mu^2 = -\frac{M_Z^2}{2} + \frac{m_{H_d}^2 - m_{H_u}^2 \tan^2 \beta}{\tan^2 \beta - 1} + \frac{h_t^2 \sin^2 \beta}{\cos 2\beta} (X_1 + X_2) + \mathcal{O}(h_t \lambda, G^2), \quad (33)$$

$$B_\mu = (m_{H_d}^2 + m_{H_u}^2 + 2\lambda^2 v_N^2) \frac{\sin 2\beta}{2} + \frac{1}{2} h_t^2 \sin 2\beta (X_1 + X_2) + \mathcal{O}(h_t \lambda, G^2), \quad (34)$$

$$2\kappa^2 v_N^2 = \lambda v^2 (\kappa \sin 2\beta - \lambda) - m_N^2 + A_\lambda \lambda v^2 \frac{\sin 2\beta}{2v_N} + \kappa A_\kappa v_N + \mathcal{O}(h_t \lambda, G^2). \quad (35)$$

here

$$G^2 = g_Y^2 + g_2^2, \quad (36)$$

$$X_i = \frac{3}{32\pi^2} \left[2 \left(\ln \frac{m_{\tilde{t}_i}^2}{\Lambda_{\overline{\text{MS}}}^2} - 1 \right) m_{\tilde{t}_i}^2 \right] \quad (37)$$

with $i = 1, 2$. Typically we have

$$m_{\tilde{t}_{1,2}}^2(\Lambda_{\overline{\text{MS}}}) \gg \Lambda_{\overline{\text{MS}}}^2 \quad (38)$$

if $\Lambda_{\overline{\text{MS}}} \sim m_t$ is assumed, which leads to

$$\begin{aligned} X_1 + X_2 &\sim 10^{-2}(m_{\tilde{Q}_3}^2(\Lambda_{\overline{\text{MS}}}) + m_t^2(\Lambda_{\overline{\text{MS}}})) \\ &\sim (100\text{GeV})^2, \end{aligned} \quad (39)$$

for the soft masses $m_{\tilde{Q}_3}^2(\Lambda_{\overline{\text{MS}}})$ and $m_t^2(\Lambda_{\overline{\text{MS}}})$ of $(\text{TeV})^2$ order. Given $\frac{h_t^2 \sin^2 \beta}{\cos 2\beta} < 0$ for $\tan \beta > 1$, the dominant effect of $\frac{m_{H_d}^2 - m_{H_u}^2 \tan^2 \beta}{\tan^2 \beta - 1}$ in mediating μ^2 therefore is weakened by the one-loop corrections. It turns out that, for an effective $\mu = \lambda v_N$ as small as 100GeV, the EW scale can still be stabilized and phenomenologically interesting physics can still arise (See Tables (1)-(8)). More results from the numerical analysis will be given in the next section.

3 Numerical Analysis

The general gauge mediation contains four unknown input parameters: the superpotential couplings $\lambda(\Lambda_{EW})$ and $\kappa(\Lambda_{EW})$, the messenger scale Λ_M and the ratio of the two effective SUSY breaking scales $\eta = \Lambda_l/\Lambda_q$. All soft SUSY-breaking parameters at the EW scale can be obtained by solving the RG equations summarized in the Appendix A, with the boundary conditions at the messenger scale Λ_M given by Eqs.(28)-(29). As for the Yukawa couplings h_t and h_b , even though we need to give them initial values while minimizing the Higgs potential, these values must be consistent with the masses of the top and bottom quarks or the output values of v_d and v_u ³. So they are not true input parameters.

The introduction of the new parameter η can lead to several different phases after EW symmetry breaking:

(A) For fixed λ , κ and Λ_M , if choose $\eta \sim 1$, we recover the GFM phase discussed in [7]. As explained above, this phase does not generate correct physics consistent with the current experimental bounds [7].

(B) With a further increased η , a new kind of phase with $v_d = v_N = 0$ and $v_u \neq 0$ may appear. Actually, this phase has been noticed in a different background [10].

(C) We will refer to the third kind of phase as “physical μ/B_μ phase”. As η increases, v_N becomes large compared to $v = \sqrt{v_d^2 + v_u^2} = 174\text{GeV}$. As a result, one can always find an η window characterized by $v_N \gg v$ where the phenomenologically interesting physics can be generated. Such η windows will be our focus in this paper. Explicitly, we will study such physical η windows corresponding to different points in the parameter space expanded by the other three input parameters: λ , κ and Λ_M .

(D) If η keeps increasing, we will meet the last phase which is characterized by $v_N \neq 0$ and

³In the numerical work, we use the tree level relationship

$$h_t \approx \frac{165\text{GeV}}{v_u}, \quad h_b \approx \frac{h_t \tan \beta}{55} \quad (40)$$

where we have identified the running top-quark mass by applying the appropriate QCD corrections to the top quark pole mass, and the running mass of m_b at the EW scale has been taken to be about 3 GeV.

$v_d = v_d = 0$. This is caused by large, negative $m_N^2(\Lambda_{EW})$. In this case, the RG evolution of $m_{H_u}^2$ to negative values is highly suppressed by the negative m_N^2 as well as the masses of the EW gauginos.

The appearing of the multiple phases reflects the large freedom degree caught by the parameter η . In the following we will focus on the physics in the physical η windows.

Our numerical results are summarized in Tables(1)-(8) which correspond to three typical cases in the phase (C) discussed above: low-scale ($\Lambda_M \sim 10^5 - 10^6 \text{ GeV}$), intermediate-scale ($\Lambda_M \sim 10^{11} \text{ GeV}$) and high-scale ($\Lambda_M \sim 10^{15} \text{ GeV}$) general gauge mediation⁴. We choose nine points on the $\lambda(\Lambda_{EW}) - \kappa(\Lambda_{EW})$ plane, and then study their physics in all of the three cases which in turn helps us figure out the related η windows. The numerical results show that to obtain consistency with current phenomenological bounds, relatively small values of η , $\eta \sim 2$, are required in the low-scale general gauge mediation. This should be compared with values of $\eta \sim 4$ for the intermediate-scale case and $\eta \sim 5$ for the high-scale case.

This can be simply understood in the following way. As the path length of the RG evolutions increases (due to the increase of Λ_M), $m_{H_u}^2$ runs towards negative values at the late stage of its evolution. This makes the beta function of m_N^2 very small or even negative. As a result, one cannot obtain large enough negative values of $m_N^2(\Lambda_{EW})$. A larger η can help solve this problem, since it implies a smaller beta function for $m_{H_u}^2$, preventing $m_{H_u}^2$ from becoming negative too fast.

Actually, the present experimental bounds lead to a more complicated than the simple picture presented above. In this model, the main constraints are from the lightest chargino mass or the lightest CP -even Higgs mass, depending on the messenger scale Λ_M . For $M_2(\Lambda_{EW}) \gg \mu > m_W$ (as typically happens in this model), the lightest chargino mass is given by

$$m_{\chi_1^c} = \mu + \mathcal{O}\left(\frac{\mu}{M_2}, \frac{m_W}{M_2}\right). \quad (41)$$

As for the lightest CP -even Higgs, it is typically H_u -like (because of the small mixing due to a not large $A_\lambda(\Lambda_{EW})$ soft term). Its mass square at the tree level is known to be typically less than m_Z^2 , so the one-loop corrections need to be included to escape the experimental bound. In all the models we analyzed, the would be MSSM CP -odd Higgs boson becomes very heavy and the lightest CP -even Higgs mass is affected by a potentially large mixing with the CP -even singlet state. As we will discuss below, $\tan \beta$ also becomes large in these models. The resulting formula for the one-loop corrected Higgs mass in the limit $v_N \gg v$ and large $\tan \beta$, and ignoring effects proportional to the relatively small stop mixing parameter is given by

$$m_{h_1}^2 = M_Z^2 - \frac{\lambda^4}{\kappa^2} v^2 + \delta m_{h_1}^2 + \mathcal{O}\left(\frac{v^4}{m_A^4}, \frac{1}{\tan \beta^2}\right), \quad (42)$$

⁴Some recent papers point out that [14]: in the context of $SU(5)$ gauge mediation, the requirement of a light gravitino as dark matter favors the intermediate-scale scenario. In this paper we will not expand this issue, but leave the associated discussions to future work.

$$\delta m_{h_1}^2 = \frac{3m_t^4}{4\pi^2 v^2} \ln \left(\frac{\sqrt{m_{\tilde{t}_1}^2 m_{\tilde{t}_2}^2}}{m_t^2} \right) + \mathcal{O} \left(h_t^2 g^2, h_t^2 \lambda^2, \frac{A_t^2}{\sqrt{m_{\tilde{t}_1}^2 m_{\tilde{t}_2}^2}} \right). \quad (43)$$

Here m_t is the running top quark mass at the top-quark mass scale and

$$m_A^2 = \frac{2\mu(A_\lambda + \frac{\kappa}{\lambda}\mu) + \delta_A}{\sin 2\beta} \quad (44)$$

is the would-be MSSM CP -odd Higgs boson mass, with

$$\begin{aligned} \delta_A \approx & \frac{3}{16\pi^2} \frac{h_t^2 A_t \mu}{m_{\tilde{t}_1}^2 - m_{\tilde{t}_2}^2} \left[m_{\tilde{t}_1}^2 \left(\ln \frac{m_{\tilde{t}_1}^2}{m_t^2} - 1 \right) - m_{\tilde{t}_2}^2 \left(\ln \frac{m_{\tilde{t}_2}^2}{m_t^2} - 1 \right) \right] \\ & + \frac{3}{16\pi^2} \frac{h_b^2 A_b \mu}{m_{\tilde{b}_1}^2 - m_{\tilde{b}_2}^2} \left[m_{\tilde{b}_1}^2 \left(\ln \frac{m_{\tilde{b}_1}^2}{m_t^2} - 1 \right) - m_{\tilde{b}_2}^2 \left(\ln \frac{m_{\tilde{b}_2}^2}{m_t^2} - 1 \right) \right] \end{aligned} \quad (45)$$

being a one loop correction factor. Observe that we have omitted the positive tree-level term proportional to $\lambda^2 \sin^2 2\beta$, which becomes unimportant for large values of $\tan \beta$, and we have included the more important contribution coming from the mixing with the singlet state, that in the limit we are working becomes independent of the mass parameters of the theory. This occurs since the singlet CP -even state acquires a mass about $4\kappa^2 v_N^2$ and its mixing matrix element with the lightest MSSM CP -even Higgs state is approximately equal to $2\lambda^2 v_N v$ in this limit. Note also that within this approximation, the $\mathcal{O}(m_t^4)$ loop correction is independent of the renormalization scale $\Lambda_{\overline{\text{MS}}}$, and is determined by the geometric average of the two stop mass squares.

For the low-scale general gauge mediation, the RG evolution paths of the stop soft masses $m_{\tilde{Q}_{3L}}^2$ and $m_{\tilde{t}_R}^2$ are short. Given the effective SUSY breaking scales $\Lambda_q \sim \Lambda_l \sim (10^5 - 10^6)$ GeV, $m_{\tilde{t}_1}^2$ and $m_{\tilde{t}_2}^2$, and hence $\delta m_{h_1}^2$ could be large according to Eq.(43). In such cases (see points A2, A3, A4, A6 and A7, and also see points B4 and C4 in the intermediate- and high-scale cases, respectively), the main constraint on the model comes from the lightest chargino mass $m_{\chi_{\tilde{1}}}$ which currently is bounded to be larger than 103.5 GeV [15]. As emphasized above, to generate a large chargino mass or effective μ , we need to modify the relative velocities of the RG evolutions of $m_{H_u}^2$ and m_N^2 . With η shifted from ~ 1 to ~ 2 , the RG evolution of $m_{H_u}^2$ to a negative value is slowed down, but that of m_N^2 is speeded up. A negative enough $m_N^2(\Lambda_{EW})$ and hence a large enough μ are generated. For the intermediate- or high-scale cases, because of the increased path length of its RG evolution and the positivity of its beta function, $m_{\tilde{t}_R}^2(\Lambda_{EW})$ becomes relatively small, leading to a small $\delta m_{h_1}^2$. In these two cases (also see points A1, A5, A8 and A9 in the low-scale case), therefore, the main constraint on the model comes from the lightest CP -even Higgs mass which currently is bounded by 114.4 GeV [16]. It is easy to see according to Eq.(42) that a small λ and a large κ is helpful in obtaining a large h_1 mass. Let us stress that in the numerical calculations of this paper, only the dominant one-loop corrections to the Higgs effective potential have been included. One should worry about the latent negative effects

on the Higgs masses from the higher-loop corrections which may shift down the mass of the lightest CP -even Higgs by several GeVs, similar to what happens in the MSSM (e.g., see [17]). These negative effects may push the lightest CP -even Higgs boson to values below the current experimental bound. This can be compensated, within our model, by a slight shift in η and a corresponding shift upwards of the superparticle masses.

The general gauge mediation model discussed in the present work favors heavy scalars and gauginos, as well as large values of $\tan\beta$: $5 \sim 50$. The heaviness of the scalars and gauginos of the theory is a reflection of the large values of the effective SUSY breaking scales $\Lambda_{q,l}$ necessary to fulfill the Higgs and/or chargino mass constraints. The preference for large values of $\tan\beta$ can be easily understood by analyzing the minimization conditions. First of all, B_μ is relatively small because the boundary value of the soft parameter A_λ at the messenger scale is highly suppressed in our model. Then, since the term $m_{H_d}^2(\Lambda_{EW}) + m_{H_u}^2(\Lambda_{EW})$ in Eq.(34) is typically larger than the other terms in Eq.(34) (see Table(1), (3), and (5)), only a relatively large $\tan\beta$ can suppress the RHS of Eq.(34) to make it match with a small B_μ . The precise value of $\tan\beta$ depends on the messenger scale. A higher messenger scale Λ_M generally leads to a more negative $m_N^2(\Lambda_{EW})$ because of the extended RG evolution path (actually, the enlarged beta function of m_N^2 due to a larger η required by phenomenology also has a contribution.) or a larger κv_N according to Eq.(35). According to Eq.(18) and Eq.(34), this indicates a larger B_μ or equivalently, a smaller $\tan\beta$. Therefore, for fixed λ and κ , $\tan\beta$ becomes smaller as Λ_M increases. On the other hand, for fixed Λ_M , a larger $\tan\beta$ often implies a larger λ or a smaller κ . For fixed κ , a larger λ implies a larger beta function for m_N^2 or a more negative $m_N^2(\Lambda_{EW})$, so a smaller $\tan\beta$ can be explained according to the same argument as that in case. For fixed λ , a smaller κ implies a larger v_N or B_μ according to Eq.(35) and Eq.(18). This then leads to a smaller $\tan\beta$ again according to Eq(34).

A large $\tan\beta$ is welcomed in phenomenology, due to its role in explaining the mass hierarchy of top and bottom quarks or realizing the unification of their Yukawa couplings (e.g., see [18]). In our model, relatively large values of $\tan\beta$ bring us more than that, since it helps in avoiding an unacceptably light chargino: in the mass formula of the lightest chargino Eq.(41), the corrections at the order $\mathcal{O}(\frac{\mu}{M_2})$ contain a negative contribution

$$\mathcal{O}\left(\frac{\mu}{M_2}\right) \simeq -\frac{2\mu}{|M_2|}m_W^2 \sin 2\beta, \quad (46)$$

which is suppressed by a large $\tan\beta$. Moreover, a relatively large $\tan\beta$ plays a crucial role in the solution of the light $U(1)_R$ pseudoscalar problem.

As first pointed out in [6], small $|A_\lambda(\Lambda_{EW})|$ and $|A_\kappa(\Lambda_{EW})|$ (compared to Λ_{EW}) induce the presence of a light pseudoscalar. In this limit, the mass of the lightest CP -odd Higgs boson is approximately given by (e.g., see [19]):

$$m_{a_1}^2 = 3v_N \left(\frac{3\lambda A_\lambda \cos^2 \theta_A}{2 \sin 2\beta} + \kappa A_\kappa \sin^2 \theta_A \right) + \mathcal{O}\left(\frac{A_\lambda}{v}, \frac{A_\kappa}{v}\right), \quad (47)$$

where

$$a_1 = \cos \theta_A A_{MSSM} + \sin \theta_A A_N \quad (48)$$

with A_{MSSM} and A_N being the doublet and singlet CP -odd gauge eigenstates, respectively, and $0 \leq \theta_A \leq \frac{\pi}{2}$ being their mixing angle. Depending on its composition, a light pseudoscalar may be in conflict with the strong LEP bounds. As extensively discussed in the literature, this light pseudoscalar should be understood as the Nambu-Goldstone boson of the global $U(1)_R$ symmetry, since $A_\lambda(\Lambda_{EW})$ and $A_\kappa(\Lambda_{EW})$ represent the only two terms explicitly violating this symmetry. However, from Table (1)-(8), it is easy to see that there is no such a problem in our model: for the intermediate- and high-scale gauge-mediations, $|A_\lambda(\Lambda_{EW})|$ is typically large, compared to Λ_{EW} ; for the low-scale case, even though $|A_\lambda(\Lambda_{EW})|$ and $|A_\kappa(\Lambda_{EW})|$ are small (except point A8), the light pseudoscalar is extremely singlet-like (see Table(7)), escaping the experimental constraints successfully.

These features are due to η and the relatively large $\tan\beta$ again. Consider the strongly coupled RG evolutions of A_t , A_b and A_λ (see RG equations (A.12), (A.13) and (A.15)). At the messenger scale we have $A_t(\Lambda_M) \sim A_b(\Lambda_M) \sim A_\lambda(\Lambda_M) \sim 0$ in our model. A larger η implies more negative contributions to the beta functions according to the EW gaugino soft masses, and less negative contributions according to the gluino soft mass. Since the latter is absent in the beta function of A_λ , but contributing to those of A_t and A_b , a large η necessarily leads to a larger $A_\lambda(\Lambda_{EW})$, as long as the evolution pathes are long enough. This explains the relatively large $A_\lambda(\Lambda_{EW})$ and large $U(1)_R$ pseudoscalar masses in the contexts of the intermediate- and high-scale general gauge mediations. Unlike these two cases, the $U(1)_R$ pseudoscalar is still light in the low-scale case (except point A8) due to the short RG evolution path for A_λ . A relatively large $\tan\beta$ plays a crucial role in avoiding the experimental bound here. As shown in [19], the mixing angle θ_A of the $U(1)_R$ pseudoscalar a_1 satisfies

$$\tan\theta_A = \frac{v_N}{v \sin 2\beta} + \mathcal{O}\left(\frac{A_\lambda}{v}, \frac{A_\kappa}{v}\right) \quad (49)$$

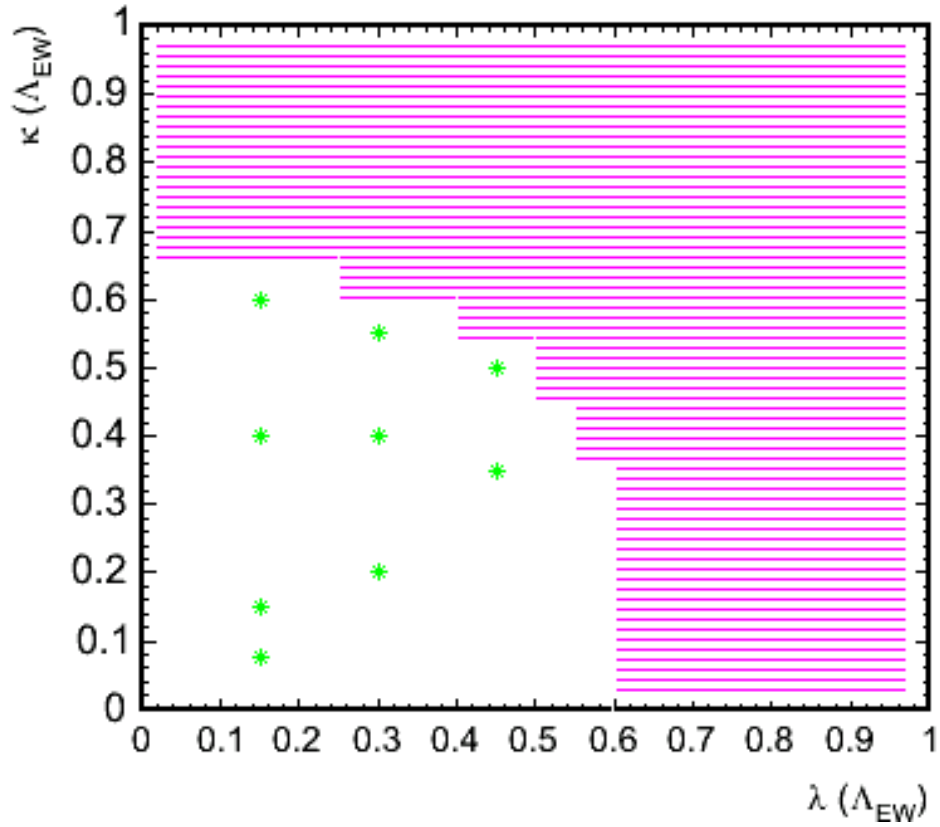
under the limit of small $A_\lambda(\Lambda_{EW})$ and $A_\kappa(\Lambda_{EW})$. Obviously, a relatively large $\tan\beta$ implies

$$\theta_A \approx \frac{\pi}{2} \quad (50)$$

and hence an extremely singlet-like $U(1)_R$ pseudoscalar a_1 (see Table(7)). This is also true for the few examples in the intermediate-scale general gauge mediation (points B1, B2 and B3 in Table (7)). The light $U(1)_R$ pseudoscalar problem, therefore, is no longer a problem in our model.

To end this section, let us take a look at the possible range of λ and κ at the EW scale in the NMSSM. The most serious constraint is from the requirement of λ and κ to be perturbative up to the GUT scale. For the case where the gauge couplings are the only possible tree-level interactions between the observable and messenger sectors, the boundary between the perturbative and non-perturbative regions has been drawn in Fig.(1), with $h_t(\Lambda_{EW}) = 0.95$, $h_b(\Lambda_{EW}) = 0.5$ and $\Lambda_M = 10^{11}$ GeV. From the figure, it is easy to see that both large $\lambda(\Lambda_{EW})$ and large $\kappa(\Lambda_{EW})$ regions have been excluded, and the only allowed region is located in the lower-left corner of the $\lambda(\Lambda_{EW}) - \kappa(\Lambda_{EW})$ plane. The boundary in the figure depends on the Yukawa couplings as well as the messenger scale. But this dependence

Figure 1: Boundary between the perturbative and the non-perturbative regions on the $\lambda(\Lambda_{EW}) - \kappa(\Lambda_{EW})$ plane. In the perturbative region (blank one), λ and κ keep perturbative up to the GUT scale. The stars on the plane denote the sample points we are studying. The boundary has a weak dependence on Yukawa couplings and the messenger scale. Here we set $h_t(\Lambda_{EW}) = 0.95$, $h_b(\Lambda_{EW}) = 0.5$ and $\Lambda_M = 10^{11}$ GeV.



is very weak: there is only a mild shift as these parameters vary in the region in which we are interested. The stars on the $\lambda(\Lambda_{EW}) - \kappa(\Lambda_{EW})$ plane denote the sample points we are studying in this paper. It is easy to see that these points cover almost the whole perturbative region on the $\lambda(\Lambda_{EW}) - \kappa(\Lambda_{EW})$ plane. In particular, all of them lead to reasonable particle mass spectra which satisfy the current experimental bounds⁵. Therefore, the μ/B_μ problem is solved in the context of the general gauge mediated SUSY breaking model analyzed in this work.

4 Collider Signals

Although a detailed analysis of the collider signatures of these models is beyond the scope of this article, we would like to stress some relevant properties of these models and their associated phenomenology.

For the low scale gauge mediation, all colored particles are very heavy and therefore very difficult to detect at hadron colliders. One promising way to test these models is by analyzing the production and two-body decay of the next-to-lightest superparticle (NLSP) to gravitino (\tilde{G}^α) which is described by

$$\mathcal{L} \sim \frac{1}{F} \partial_\mu G^\alpha j_\alpha^\mu + h.c., \quad (51)$$

Here \sqrt{F} is the SUSY breaking scale, and j_α^μ is the supercurrent. In our model, the NLSP generally is the lightest neutralino which is typically Higgsino-like, and in most cases whose mixing with singlino is suppressed (see Table(8) for the case with low-scale gauge mediation). So the most important experimental signature would be the di- Z and di- h_1 productions (if allowed by phase space)

$$\begin{aligned} \chi_1^0 &\rightarrow Z\tilde{G} : & ZZ + X + \cancel{E} \\ \chi_1^0 &\rightarrow h_1\tilde{G} : & h_1h_1 + X + \cancel{E} \end{aligned} \quad (52)$$

here X is any collection of leptons and jets, and \cancel{E} denotes the missing energy. Explicitly, under the Higgsino-like limit (with the mixing with the singlino suppressed), the decay rates to Z -boson and h_1 are given by [20]

$$\begin{aligned} \Gamma(\chi_1^0 \rightarrow Z\tilde{G}) &\approx \frac{1}{2} |c_{\tilde{H}_d} \cos \beta + c_{\tilde{H}_u} \sin \beta|^2 \frac{m_{\chi_1^0}^5}{16\pi F^2} \left(1 - \frac{m_Z^2}{m_{\chi_1^0}^2}\right)^4, \\ \Gamma(\chi_1^0 \rightarrow h_1\tilde{G}) &\approx \frac{1}{2} |c_{\tilde{H}_d} \sin \alpha - c_{\tilde{H}_u} \cos \alpha|^2 \frac{m_{\chi_1^0}^5}{16\pi F^2} \left(1 - \frac{m_{h_1}^2}{m_{\chi_1^0}^2}\right)^4. \end{aligned} \quad (53)$$

⁵Actually, if the requirements of perturbativity (up to Λ_{GUT}) for the couplings are given up, the nice features of these examples could be extended into the non-perturbative region on the $\lambda(\Lambda_{EW}) - \kappa(\Lambda_{EW})$ plane as long as these couplings stay perturbative at the messenger scale.

Here $c_{\tilde{H}_d}$ and $c_{\tilde{H}_u}$ are composition coefficients of χ_1^0 , and α is the $h_1 - h_2$ Higgs mixing angle. If the singlino component of χ_1^0 is not small, e.g., at A1 point, the di- a_1 decay can also provide useful collider signals. Note that in our model independently of that $\langle S_q \rangle \sim \langle S_l \rangle \sim \Lambda_M$ or $\langle S_q \rangle \sim \eta \langle S_l \rangle \sim \Lambda_M^2 / \langle S_l \rangle$ is assumed, we typically have $\sqrt{F} \sim \sqrt{F_q F_l}$ between a few 10^5 GeV and a few 10^6 GeV, which implies non-prompt di-boson decays [21]. This is important since the background for any of the final state signatures can be greatly reduced (due to the displaced vertices and distinguished angular distribution of the displaced jets from Z or h_1 decays) if the χ_L^0 decay is non-prompt but contained in the tracking region.

It is also important to stress that in the low scale gauge mediated scenario, the Higgs decays may be affected by the presence of the light pseudoscalars, a_1 . Although the lightest pseudoscalar is mostly a singlet state (see Table 7), it will decay into bottom quark and τ pairs through its mixing with the pseudoscalar component of the Higgs doublet H_d . Therefore, the Higgs decay into two a_1 states will induce decays into either four bottom quarks, two bottom quark and two τ 's, or four τ 's final states. The final signatures of the di- h_1 channel in 52, necessarily, will also be affected. In all the scenarios we presented, the lightest CP-even Higgs is sufficiently heavy as to evade the stringent LEP constraints on a light CP-even Higgs decaying into four bottom quark final states [28]. The presence of these new decay channels will demand new strategies for the search for CP-even Higgs bosons at the Tevatron and the LHC, as has been recently analyzed in Refs. [29].

The gravitino collider signals are seriously suppressed for intermediate- and high-scale gauge mediations, since the neutralino lifetime will be enhanced by the factor F^2 and therefore it will decay beyond the detector. Moreover, whenever light, the charged and neutral Higgsinos would be approximately degenerate in mass and therefore difficult to detect by direct production at hadron colliders. However, colored particles become lighter and therefore they provide the most important search channels at the LHC. In the high-scale case, the gluino mass $m_{\tilde{g}}$ is typically around 1.5 TeV or even smaller, implying an abundant production of gluinos at LHC, according to the gluino (\tilde{g}) pair production

$$pp \rightarrow \tilde{g}\tilde{g}. \quad (54)$$

Meanwhile, given that the lightest stop \tilde{t}_1 is mainly right-handed and much lighter than gluino in this case, one could expect to see the signatures at LHC according to the decaying channels

$$\begin{aligned} \tilde{g} &\rightarrow \tilde{t}_1 \rightarrow t\chi_1^0, \\ \tilde{g} &\rightarrow \tilde{t}_1 \rightarrow t\chi_1^c. \end{aligned} \quad (55)$$

Therefore, the final state will be given by four top quarks or two top and two bottom quarks with large missing energy. An analysis of similar gluino decay channels at the LHC has been performed in Ref. [30]. Even though we typically have $m_{\chi_1^0} < m_{\tilde{t}_1}$ in the high-scale scenario, C9 point is an exception, where \tilde{t}_1 is lighter than χ_1^0 and $\tilde{\tau}_1$. The light stop \tilde{t}_1 is long-lived because its two-body decay to gravitino

$$\tilde{t}_1 \rightarrow t\tilde{G}, \quad (56)$$

even if kinematically allowed, is also suppressed by a F^{-2} factor. In such a case, the stop may have interesting implications on both cosmology and collider signatures. For more details, readers may refer to [31].

As for the intermediate-scale scenario, even though an abundant production of gluinos at LHC is also expected for many cases, the mass of the lightest stop is typically larger than that of gluinos. Whenever the gluino mass is within kinematic reach of the LHC, they will decay only through off-shell squarks

$$\tilde{g} \rightarrow qq'\chi_i^0, \quad \tilde{g} \rightarrow qq'\chi_i^c. \quad (57)$$

Since the neutralinos and charginos appearing in the intermediate states have multiple decay modes, there will be many competing gluino decay chains whose branching ratios are quite sensitive to the parameters of this model. Interested readers may refer to [32] and its references.

5 Discussions and Conclusions

The general gauge mediation provides a simple way to solve the μ/B_μ problem in the NMSSM. In this context, reasonable values for μ/B_μ can be generated by properly modifying the RG evolutions of $m_{H_u}^2$ and m_N^2 by a choice of η window. The EW scale is then stabilized, and phenomenologically interesting spectra of particles and superparticles are also achieved. These features apply to most of the perturbative (up to the GUT scale) $\lambda - \kappa$ parameter region in the NMSSM and to all phenomenologically interesting messenger scales. In addition, there is no light $U(1)_R$ pseudoscalar problem in our model. For the intermediate- and high-scale gauge-mediations, due to a relatively heavy spectrum of gauginos, large $|A_\lambda(\Lambda_{EW})|$ or $|A_\kappa(\Lambda_{EW})|$, comparable with Λ_{EW} are typical, so the lightest Higgs pseudoscalar is not too light. For the low-scale case, even though $|A_\lambda(\Lambda_{EW})|$ and $|A_\kappa(\Lambda_{EW})|$ are not always large, the lightest Higgs pseudoscalar is extremely singlet-like due to a relatively large $\tan\beta$ favored by our model, escaping the experimental constraints on a light Higgs boson.

It is worth emphasizing that the introduction of the parameter η does not affect the successful prediction of the gauge coupling unification at the GUT scale. Recall the threshold corrections to the gauge coupling unification due to the little hierarchy between the EW scale and the soft SUSY breaking scale, where $\frac{\Lambda_{soft}}{\Lambda_{EW}} \sim 10$ and many charged particle species are involved. In the general gauge mediation scenario described in this article, the correction to the prediction of $\alpha_3(M_Z)$ induced by the messenger threshold corrections may be estimated by

$$\Delta\alpha_3(M_Z) \simeq \frac{9}{14\pi} \alpha_3(M_Z)^2 \ln \left(\frac{\langle S_q \rangle}{\langle S_l \rangle} \right) \quad (58)$$

On the other hand, the introduction of η also modifies the sparticle threshold corrections,

which are approximately given by [22]

$$\begin{aligned}\Delta\alpha_3(M_Z) &\simeq -\frac{19}{28\pi}\alpha_3(M_Z)^2\ln\left(\frac{|\mu|}{M_Z}\left(\frac{M_2}{M_3}\right)^{3/2}\right) \\ &= -\frac{19}{28\pi}\alpha_3(M_Z)^2\ln\left(\frac{|\mu|}{M_Z}\left(\frac{\eta\alpha_2}{\alpha_3}\right)^{3/2}\right)\end{aligned}\quad (59)$$

One could compute the difference in the prediction of $\alpha_3(M_Z)$ with respect to the case $\eta = 1$. Let us consider two cases. In the first one, the ratio of effective SUSY breaking scales $\Lambda_l/\Lambda_q \sim \langle F_l \rangle/\langle F_q \rangle \simeq \eta$, and therefore $\langle S_q \rangle/\langle S_l \rangle \sim 1$. In such a case,

$$\Delta_\eta\alpha_3(M_Z) \simeq -\frac{57}{56\pi}\alpha_3^2(M_Z)\ln\eta. \quad (60)$$

Alternatively, one can consider $\langle F_q \rangle \sim \langle F_l \rangle$ and therefore $\langle S_q \rangle/\langle S_l \rangle \simeq \eta$. In this case,

$$\Delta_\eta\alpha_3(M_Z) \simeq -\frac{21}{56\pi}\alpha_3^2(M_Z)\ln\eta. \quad (61)$$

In both cases, the total correction is negative, leading, for $\eta \simeq 2-6$ to a somewhat better agreement between the predicted and measured values of $\alpha_3(M_Z)$ than in the $\eta = 1$ case ⁶.

One interesting feature on this model is the arising of one physical CP -phase according to the gaugino soft masses. In the NMSSM with general gauge mediation, there are four independent complex parameters: λ , κ , and two of the soft gaugino masses M_1 , M_2 and M_3 . Among them, the phase of λ is not physical and can be resolved by the CKM matrix. In addition, κ and gaugino soft mass are not invariant under the Peccei-Quinn symmetry and $U(1)_R$ symmetry, respectively. The phase of κ and one phase in the gaugino mass sector hence can be rotated away. So there is one physical phase left in the soft mass sector of gauginos. On the other hand, it is well-known that the CKM phase is not enough and extra CP -violating sources are required to explain the origin of the baryon asymmetry in the Universe today. The physical CP phase appearing in our model may provide a nice chance to understand this cosmic mystery. For example, in the EW baryogenesis mechanism (see [23] for a review or [24] for its realization in different supersymmetric models), such a phase may induce a net amount of left-chiral weak fermions during the EW phase transition, which is then switched to the baryon asymmetry in the Universe according to the EW sphaleron effect. But, the same as the CP phases appearing in any other supersymmetric models, the physical CP -phase in our model also needs to satisfy the EDM bounds of electron, neutron and mercury atoms. Since the masses of the first two family squarks in our model are typically heavier than 2–3 TeV, it might be viable to suppress its one-loop contributions to the EDMs according to the heavy squark mechanism [25]. In addition, it is claimed recently [26] that in a context similar to ours, a large CP -phase of order $\mathcal{O}(1)$ can be consistent with all EDM bounds according to some cancellation effects, with no necessity to require the squarks of the first two families to be heavy.

⁶Successful unification in the $\eta = 1$ case requires the threshold scale $|\mu|(\alpha_2/\alpha_3)^{3/2} \simeq 1TeV$.

It is interesting to ask why the situation is so different between the class of models [8, 10] and our model, since both of them have a total of four free input parameters, with one messenger coupling in the former case replaced by the parameter η in our model. To great extent this is due to the different ways in which the negative soft mass square $m_N^2(\Lambda_{EW})$ is generated. In the former case, the authors try to generate a negative $m_N^2(\Lambda_{EW})$ directly according to the boundary conditions at the messenger scale. They let the singlet \mathbf{N} directly couple to the messengers. Then, the contribution of this coupling to $m_N^2(\Lambda_M)$ at two-loop level are negative. But this coupling has similar negative contributions to $m_{H_u}^2(\Lambda_M)$ making $m_{H_u}^2$ get enough negative values quickly to induce EW symmetry breaking. This in turn refrains m_N^2 from getting a too negative value at the EW scale according to the RG evolution. In our model, we try to generate a negative $m_N^2(\Lambda_{EW})$ by modifying the related RG evolutions. The introduced parameter η have opposite effects on the beta functions $m_{H_u}^2$ and m_N^2 , so the evolution of m_N^2 to a negative value is accelerated while that of $m_{H_u}^2$ is slowed down. This allows m_N^2 have enough time to obtain a very negative value before $m_{H_u}^2$ induces the EW symmetry breaking. In addition, unlike the former case, the trilinear soft parameters A_λ and A_κ are highly suppressed at the messenger scale, which leads to a relatively large $\tan\beta$ at the EW scale. This relatively large $\tan\beta$ not only helps lift the mass of the lightest chargino, but more importantly, help solve the light $U(1)_R$ pseudoscalar problem by suppressing its mixing with the SM-like CP -odd Higgs components.

The general gauge mediation is natural because of its simplicity and universality. It is very simple, only requiring minimal messenger spectrum in the messenger sector and with no additional symmetry or new dimensional parameters introduced. Most importantly, it can naturally arise from a general hidden sector, as pointed out in subsection 2.2. Since the construction of this model is independent of the visible sector, its idea can also be extended to many other contexts without much difficulty, e.g., the nMSSM and the UMSSM, or even help the class of models in [8, 10] obtain more reasonable physical results. Due to the similar structures of the related beta functions, we believe that similar effects could be seen in these extensions. We will leave these interesting issues to future exploration.

Acknowledgments

We would like to thank André de Gouvêa, John Gunion, Paul Langacker, Arjun Menon and David Morrissey for useful discussions and comments. Work at ANL is supported in part by the U.S. Department of Energy (DOE), Div. of HEP, Contract DE-AC02-06CH11357. Work at EFI is supported in part by the U.S. DOE through Grant No. DEFG02-90ER40560. T.L. is also supported by Fermi-McCormick Fellowship.

Appendix A The RG Equations in the NMSSM

All of the one-loop RG equations in the NMSSM (e.g., see [27]) are listed in this section. Considering that the beta functions of RGEs in a general background also depend on the couplings between the observable sector, and the messenger and hidden sectors, here we assume that at tree-level there is no couplings between the observable and the hidden sector, and the gauge couplings are the only possible interactions between the observable and the messenger sector. In addition, in the numerical work of this paper, we neglect all threshold corrections to the RG evolutions caused by the little hierarchy between the EW scale (~ 100 GeV) and the soft SUSY breaking scale (~ 1000 GeV).

I. The sector of superpotential couplings

$$16\pi^2 \frac{d}{dt} g_Y = 11g_Y^3, \quad (\text{A.1})$$

$$16\pi^2 \frac{d}{dt} g_2 = g_2^3, \quad (\text{A.2})$$

$$16\pi^2 \frac{d}{dt} g_3 = -3g_3^3, \quad (\text{A.3})$$

$$16\pi^2 \frac{d}{dt} h_t = (6h_t^2 + h_b^2 + \lambda^2 - \frac{13}{9}g_Y^2 - 3g_2^2 - \frac{16}{3}g_3^2)h_t, \quad (\text{A.4})$$

$$16\pi^2 \frac{d}{dt} h_b = (6h_b^2 + h_t^2 + h_\tau^2 + \lambda^2 - \frac{7}{9}g_Y^2 - 3g_2^2 - \frac{16}{3}g_3^2)h_b, \quad (\text{A.5})$$

$$16\pi^2 \frac{d}{dt} h_\tau = (4h_\tau^2 + 3h_b^2 + \lambda^2 - 3g_Y^2 - 3g_2^2)h_\tau, \quad (\text{A.6})$$

$$16\pi^2 \frac{d}{dt} \lambda = (4\lambda^2 + 2k^2 + 3h_t^2 + 3h_b^2 + h_\tau^2 - g_Y^2 - 3g_2^2)\lambda, \quad (\text{A.7})$$

$$16\pi^2 \frac{d}{dt} k = 6(\lambda^2 + k^2)k. \quad (\text{A.8})$$

In the above equations $g_Y = e/\cos\theta_{EW}$ is the $U(1)_Y$ gauge coupling. In the GUT framework, it is generally normalized to be $g_1 \equiv \sqrt{\frac{5}{3}}g_Y$ and $\alpha_1 \equiv \frac{5}{3}\alpha_Y$. When $t > \ln(\frac{\Lambda_M}{\Lambda_{EW}})$, the RGEs of g_Y , g_2 and g_3 are modified to

$$16\pi^2 \frac{d}{dt} g_Y = (11 + \frac{5n}{3})g_Y^3, \quad (\text{A.9})$$

$$16\pi^2 \frac{d}{dt} g_2 = (1 + n)g_2^3, \quad (\text{A.10})$$

$$16\pi^2 \frac{d}{dt} g_3 = (-3 + n)g_3^3 \quad (\text{A.11})$$

with n being the number of messenger pairs $(3 + 2) + (\bar{3} + \bar{2})$.

II. The sector of soft A-term couplings

$$16\pi^2 \frac{d}{dt} A_{u_a} = 6h_t^2(1 + \delta_{a3})A_t + 2h_b^2\delta_{a3}A_b + 2\lambda^2 A_\lambda - 4\left(\frac{13}{18}g_Y^2 M_1 + \frac{3}{2}g_2^2 M_2 + \frac{8}{3}g_3^2 M_3\right), \quad (\text{A.12})$$

$$16\pi^2 \frac{d}{dt} A_{d_a} = 6h_b^2(1 + \delta_{a3})A_b + 2h_t^2\delta_{a3}A_t + 2h_\tau^2\delta_{a3}A_\tau + 2\lambda^2 A_\lambda - 4\left(\frac{7}{18}g_Y^2 M_1 + \frac{3}{2}g_2^2 M_2 + \frac{8}{3}g_3^2 M_3\right), \quad (\text{A.13})$$

$$16\pi^2 \frac{d}{dt} A_{e_a} = 2h_\tau^2(1 + 3\delta_{a3})A_\tau + 6h_b^2 A_b + 2\lambda^2 A_\lambda - 6(g_Y^2 M_1 + g_2^2 M_2), \quad (\text{A.14})$$

$$16\pi^2 \frac{d}{dt} A_\lambda = 8\lambda^2 A_\lambda - 4k^2 A_k + 6h_t^2 A_t + 6h_b^2 A_b + 2h_\tau^2 A_\tau - 2(g_Y^2 M_1 + 3g_2^2 M_2), \quad (\text{A.15})$$

$$16\pi^2 \frac{d}{dt} A_k = 12(k^2 A_k - \lambda^2 A_\lambda). \quad (\text{A.16})$$

Here A_i are the soft SUSY-breaking A-term couplings. M_i ($i=1,2,3$) are the soft SUSY-breaking gaugino masses which evolve as

$$M_1(t) = \frac{g_Y(t)^2}{16\pi^2} (\Lambda_l + \frac{2}{3}\Lambda_q) \quad (\text{A.17})$$

$$M_2(t) = \frac{g_2(t)^2}{16\pi^2} \Lambda_l \quad (\text{A.18})$$

$$M_3(t) = \frac{g_3(t)^2}{16\pi^2} \Lambda_q \quad (\text{A.19})$$

at one-loop level in our model.

III. The sector of soft SUSY-breaking masses

$$16\pi^2 \frac{d}{dt} m_{\tilde{Q}_a}^2 = 2\delta_{a3}h_t^2(m_{\tilde{Q}_3}^2 + m_{H_u}^2 + m_t^2 + A_t^2) + 2\delta_{a3}h_b^2(m_{\tilde{Q}_3}^2 + m_{H_d}^2 + m_b^2 + A_b^2) - 8\left(\frac{1}{36}g_Y^2 M_1^2 + \frac{3}{4}g_2^2 M_2^2 + \frac{4}{3}g_3^2 M_3^2\right), \quad (\text{A.20})$$

$$16\pi^2 \frac{d}{dt} m_{\tilde{u}_a}^2 = 4\delta_{a3}h_t^2(m_{\tilde{Q}_3}^2 + m_{H_u}^2 + m_t^2 + A_t^2) - 8\left(\frac{4}{9}g_Y^2 M_1^2 + \frac{4}{3}g_3^2 M_3^2\right), \quad (\text{A.21})$$

$$16\pi^2 \frac{d}{dt} m_{\tilde{d}_a}^2 = 4\delta_{a3}h_b^2(m_{\tilde{Q}_3}^2 + m_{H_d}^2 + m_b^2 + A_b^2) - 8\left(\frac{1}{9}g_Y^2 M_1^2 + \frac{4}{3}g_3^2 M_3^2\right), \quad (\text{A.22})$$

$$16\pi^2 \frac{d}{dt} m_{\tilde{L}_a}^2 = 2\delta_{a3}h_\tau^2(m_{\tilde{L}_3}^2 + m_{H_d}^2 + m_\tau^2 + A_\tau^2) - 8\left(\frac{1}{4}g_Y^2 M_1^2 + \frac{3}{4}g_2^2 M_2^2\right), \quad (\text{A.23})$$

$$16\pi^2 \frac{d}{dt} m_{\tilde{e}_a}^2 = 4\delta_{a3} h_\tau^2 (m_{\tilde{L}_3}^2 + m_{H_d}^2 + m_{\tilde{\tau}}^2 + A_\tau^2) - 8g_Y^2 M_1^2, \quad (\text{A.24})$$

$$16\pi^2 \frac{d}{dt} m_{H_d}^2 = 6h_b^2 (m_{\tilde{Q}_3}^2 + m_{H_d}^2 + m_b^2 + A_b^2) + 2h_\tau^2 (m_{\tilde{L}_3}^2 + m_{H_d}^2 + m_{\tilde{\tau}}^2 + A_\tau^2) \\ + 2\lambda^2 (m_{H_d}^2 + m_{H_u}^2 + m_N^2 + A_\lambda^2) - 8\left(\frac{1}{4}g_Y^2 M_1^2 + \frac{3}{4}g_2^2 M_2^2\right), \quad (\text{A.25})$$

$$16\pi^2 \frac{d}{dt} m_{H_u}^2 = 6h_t^2 (m_{\tilde{Q}_3}^2 + m_{H_u}^2 + m_t^2 + A_t^2) + 2\lambda^2 (m_{H_d}^2 + m_{H_u}^2 + m_N^2 + A_\lambda^2) \\ - 8\left(\frac{1}{4}g_Y^2 M_1^2 + \frac{3}{4}g_2^2 M_2^2\right), \quad (\text{A.26})$$

$$16\pi^2 \frac{d}{dt} m_N^2 = 4\lambda^2 (m_{H_d}^2 + m_{H_u}^2 + m_N^2 + A_\lambda^2) + 4k^2 (3m_N^2 + A_k^2). \quad (\text{A.27})$$

Here all soft SUSY-breaking masses are taken to be diagonal. Note, in all of the three sectors, only the effect of the third generation Yukawa couplings, *i.e.*, h_t , h_b and h_τ are considered.

Appendix B Numerical Results

In this section, we list the numerical results in the cases of low- (Table(1)-(2)), intermediate- (Table(3)-(4)), and high-scale (Table(5)-(6)) general gauge mediations. The composition of the light $U(1)_R$ pseudoscalar is given in Table(7), and the composition of the lightest neutralino or the NLSP in the low-scale case is given in Table(8).

Table 1: Parameters of the low-scale general gauge mediation.

	Input Parameters			
Pts	$\lambda(\Lambda_{EW})$	$\kappa(\Lambda_{EW})$	Λ_M (GeV)	η
A1	0.15	0.075	2.50×10^5	2.1160
A2	0.15	0.15	5.00×10^5	2.2708
A3	0.15	0.40	5.00×10^6	2.5151
A4	0.15	0.60	2.00×10^7	2.7869
A5	0.30	0.20	2.50×10^5	1.9356
A6	0.30	0.40	2.50×10^5	2.1383
A7	0.30	0.55	5.00×10^5	2.2800
A8	0.45	0.35	2.00×10^6	2.2509
A9	0.45	0.50	2.50×10^5	2.1083

	Soft SUSY-breaking Parameters at the EW Scale (GeV or GeV ²)						
Pts	$M_{1,2,3}$	$m_{H_d}^2$	$m_{H_u}^2$	m_N^2	A_λ	A_κ	
A1	888.7, 2225.8, 3518.0	-1.88×10^6	-7.58×10^6	-1.55×10^4	-5.0	0.7	
A2	1087.3, 2768.7, 4076.2	-5.61×10^6	-1.04×10^7	-2.24×10^4	-34.0	1.0	
A3	3561.3, 9274.7, 12311.1	-9.01×10^7	-1.18×10^8	-2.07×10^5	-268.9	5.0	
A4	3792.8, 10085.2, 12069.8	-8.80×10^7	-1.15×10^8	-3.55×10^5	-241.4	7.3	
A5	1176.0, 2881.1, 4978.1	-1.71×10^5	-1.71×10^7	-9.29×10^4	7.7	4.1	
A6	906.6, 2276.4, 3560.4	-2.63×10^6	-7.72×10^6	-5.66×10^4	-13.3	2.8	
A7	1055.3, 2689.6, 3943.7	-4.27×10^6	-9.83×10^6	-8.27×10^4	-24.0	3.8	
A8	2070.8, 5262.9, 7810.5	3.62×10^7	-5.04×10^7	-1.93×10^6	219.1	37.9	
A9	898.7, 2248.9, 3567.5	3.14×10^6	-8.05×10^6	-2.20×10^5	45.6	8.3	

	Output Parameters					
Pts	h_t, h_b	Λ_q (GeV)	$\tan\beta$	μ (GeV)	B_μ (GeV ²)	
A1	0.949, 0.753	3.90×10^5	43.57	173.8	1.41×10^4	
A2	0.948, 0.833	4.52×10^5	48.44	105.1	7.38×10^3	
A3	0.948, 0.880	1.37×10^6	51.05	121.8	6.55×10^3	
A4	0.948, 0.882	1.34×10^6	52.41	106.0	1.92×10^4	
A5	0.949, 0.637	5.46×10^5	36.93	321.8	7.11×10^4	
A6	0.948, 0.780	3.95×10^5	45.30	124.2	1.88×10^4	
A7	0.948, 0.809	4.38×10^5	46.89	109.9	1.94×10^4	
A8	0.950, 0.307	8.68×10^5	17.80	1276.6	1.54×10^6	
A9	0.949, 0.533	2.50×10^5	30.87	296.7	1.11×10^5	

Table 2: Mass spectrum of particles and superparticles in the low-scale general gauge mediation.

Particle Masses (TeV)				
Pts	$m_{\tilde{g}}$	$m_{\tilde{t}_{1,2}}$	$m_{\tilde{b}_{1,2}}$	$m_{\tilde{\tau}_{1,2}}$
A1	3.44	5.55, 6.36	5.86, 6.35	0.80, 2.84
A2	3.95	6.37, 7.36	6.60, 7.35	0.89, 3.53
A3	11.17	18.63, 22.24	19.08, 22.24	2.27, 11.90
A4	10.98	17.78, 22.18	18.26, 22.18	1.67, 12.98
A5	4.76	7.89, 8.98	8.54, 8.97	1.14, 3.69
A6	3.48	5.62, 6.42	5.89, 6.42	0.80, 2.90
A7	3.83	6.16, 7.14	6.43, 7.14	0.88, 3.43
A8	7.30	12.01, 14.72	14.15, 14.72	2.33, 6.85
A9	3.49	5.63, 6.57	6.23, 6.57	0.92, 2.88

Particle Masses (GeV)				
Pts	$m_{\chi_1^c}$	$m_{\chi_1^0}$	$m_{h_{1,2,3}}$	$m_{a_{1,2}}$
A1	173.4	155.8	118.3, 187.3, 1751.6	15.7, 1751.6
A2	105.0	103.7	136.6, 211.1, 1616.8	20.3, 1616.8
A3	121.7	121.7	152.6, 644.3, 3544.8	71.3, 3544.8
A4	106.0	105.8	152.4, 843.6, 3564.4	98.0, 3564.3
A5	321.4	311.1	117.4, 433.3, 2825.2	53.8, 2825.1
A6	123.9	119.8	133.1, 331.2, 1656.8	43.3, 1656.7
A7	109.7	107.1	137.5, 401.8, 1754.8	54.3, 1754.6
A8	1276.2	1272.4	116.2, 1973.2, 6596.7	337.4, 6596.6
A9	296.1	289.8	121.9, 659.6, 2430.1	96.1, 2429.9

Table 3: Parameters of the intermediate-scale general gauge mediation.

	Input Parameters			
Pts	$\lambda(\Lambda_{EW})$	$\kappa(\Lambda_{EW})$	Λ_M (GeV)	η
B1	0.15	0.075	1.00×10^{11}	4.180
B2	0.15	0.15	1.00×10^{11}	4.512
B3	0.15	0.40	1.00×10^{11}	4.292
B4	0.15	0.60	1.00×10^{11}	4.126
B5	0.30	0.20	1.00×10^{11}	3.981
B6	0.30	0.40	1.00×10^{11}	4.360
B7	0.30	0.55	1.00×10^{11}	4.620
B8	0.45	0.35	1.00×10^{11}	4.019
B9	0.45	0.50	1.00×10^{11}	4.542

	Soft SUSY-breaking Parameters at the EW Scale (GeV or GeV ²)					
Pts	$M_{1,2,3}$	$m_{H_d}^2$	$m_{H_u}^2$	m_N^2	A_λ	A_κ
B1	781.9, 2225.5, 1762.6	7.98×10^6	-2.23×10^6	-1.42×10^5	379.6	11.6
B2	443.3, 1274.9, 935.4	1.82×10^6	-4.37×10^5	-4.41×10^4	177.8	6.2
B3	1177.2, 3362.9, 2593.9	2.41×10^6	-4.34×10^6	-2.19×10^5	215.8	13.1
B4	2138.5, 6076.2, 4875.4	3.85×10^6	-1.76×10^7	-4.93×10^5	229.8	19.5
B5	1360.7, 3846.7, 3199.0	2.63×10^7	-9.56×10^6	-1.66×10^6	649.5	80.0
B6	762.0, 2181.3, 1656.3	7.41×10^6	-1.89×10^6	-5.00×10^5	357.5	42.7
B7	475.6, 1371.9, 983.1	2.46×10^6	-5.17×10^5	-1.73×10^5	205.9	24.4
B8	1678.7, 4752.2, 3914.6	3.95×10^7	-1.66×10^7	-5.37×10^6	730.5	214.8
B9	747.1, 2150.0, 1567.1	7.86×10^6	-1.96×10^6	-1.04×10^5	356.4	92.8

	Output Parameters				
Pts	h_t, h_b	Λ_q (GeV)	$\tan\beta$	μ (GeV)	B_μ (GeV ²)
B1	0.950, 0.331	1.98×10^5	19.11	541.4	3.51×10^5
B2	0.949, 0.550	1.05×10^5	31.88	150.3	4.91×10^4
B3	0.949, 0.780	2.91×10^5	45.17	126.0	6.92×10^4
B4	0.948, 0.832	5.47×10^5	48.15	126.2	9.22×10^4
B5	0.953, 0.183	3.59×10^5	10.57	1406.6	2.22×10^6
B6	0.949, 0.340	1.86×10^5	19.62	384.5	3.33×10^5
B7	0.949, 0.465	1.10×10^5	26.97	163.5	8.23×10^4
B8	0.957, 0.125	4.39×10^5	7.16	2188.5	5.30×10^6
B9	0.953, 0.173	1.76×10^5	10.03	673.5	7.40×10^5

Table 4: Mass spectrum of particles and superparticles in the intermediate-scale general gauge mediation.

Pts	Particle Masses (TeV)			
	$m_{\tilde{g}}$	$m_{\tilde{t}_{1,2}}$	$m_{\tilde{b}_{1,2}}$	$m_{\tilde{\tau}_{1,2}}$
B1	1.82	1.98, 4.03	3.23, 4.02	0.90, 3.07
B2	1.00	0.98, 2.16	1.56, 2.16	0.32, 1.74
B3	2.61	2.84, 5.58	3.59, 5.58	1.00, 4.49
B4	4.72	5.52, 10.16	6.42, 10.16	2.11, 8.07
B5	3.19	3.69, 7.21	6.04, 7.21	1.75, 5.34
B6	1.72	1.79, 3.86	3.02, 3.85	0.87, 3.01
B7	1.05	1.00, 2.33	1.71, 2.32	0.45, 1.88
B8	3.86	4.42, 8.87	7.44, 8.87	2.20, 6.60
B9	1.63	1.60, 3.76	2.96, 3.75	0.97, 2.98

Pts	Particle Masses (GeV)			
	$m_{\chi_1^c}$	$m_{\chi_1^0}$	$m_{h_{1,2,3}}$	$m_{a_{1,2}}$
B1	540.3	520.5	121.4, 536.5, 2931.9	97.1, 2931.9
B2	149.4	144.7	121.1, 297.6, 1416.9	54.0, 1416.9
B3	125.9	124.4	135.3, 663.8, 2367.7	115.8, 2367.6
B4	126.1	125.4	142.2, 997.6, 3227.7	172.5, 3227.6
B5	1405.5	1342.6	120.6, 1843.4, 5383.5	473.7, 5383.4
B6	383.7	380.6	126.1, 1009.0, 2803.2	192.7, 2136.1
B7	162.6	159.3	122.0, 590.0, 1623.6	150.5, 1623.3
B8	2187.3	1676.5	117.7, 3331.0, 6768.7	1045.5, 6768.5
B9	671.8	658.9	118.6, 1464.2, 2911.0	457.8, 2910.5

Table 5: Parameters of the high-scale general gauge mediation.

	Input Parameters			
Pts	$\lambda(\Lambda_{EW})$	$\kappa(\Lambda_{EW})$	Λ_M (GeV)	η
C1	0.15	0.075	1.00×10^{15}	4.695
C2	0.15	0.15	1.00×10^{15}	4.980
C3	0.15	0.40	1.00×10^{15}	5.060
C4	0.15	0.60	1.00×10^{15}	4.930
C5	0.30	0.20	1.00×10^{15}	4.639
C6	0.30	0.40	1.00×10^{15}	5.110
C7	0.30	0.55	1.00×10^{15}	5.240
C8	0.45	0.35	1.00×10^{15}	4.755
C9	0.45	0.50	1.00×10^{15}	5.560

	Soft SUSY-breaking Parameters at the EW Scale (GeV or GeV ²)					
Pts	$M_{1,2,3}$	$m_{H_d}^2$	$m_{H_u}^2$	m_N^2	A_λ	A_κ
C1	864.5, 2506.8, 1749.5	1.26×10^7	-2.73×10^6	-2.96×10^5	742.4	32.1
C2	628.2, 1834.5, 1207.0	5.67×10^6	-9.95×10^5	-1.54×10^5	498.5	22.8
C3	833.5, 2438.6, 1579.2	3.85×10^6	-1.57×10^6	-2.01×10^5	392.7	24.6
C4	1469.9, 4287.5, 2849.6	3.34×10^6	-5.76×10^6	-3.79×10^5	466.2	33.2
C5	1103.6, 3195.32, 2257.0	2.07×10^7	-5.90×10^6	-1.86×10^6	877.1	161.5
C6	742.4, 2174.7, 1394.5	9.02×10^6	-1.59×10^6	-7.82×10^5	608.1	101.4
C7	705.1, 2071.2, 1295.2	7.34×10^6	-1.24×10^6	-5.69×10^5	549.1	84.3
C8	1981.9, 5755.8, 3966.3	6.35×10^7	-2.35×10^7	-1.21×10^7	1332.5	611.7
C9	781.5, 2310.7, 1361.8	9.85×10^6	-2.04×10^6	-1.67×10^6	586.9	222.2

	Output Parameters				
Pts	h_t, h_b	Λ_q (GeV)	$\tan\beta$	μ (GeV)	B_μ (GeV ²)
C1	0.951, 0.220	1.98×10^5	12.63	792.6	8.99×10^5
C2	0.949, 0.391	1.37×10^5	22.64	285.4	2.23×10^5
C3	0.948, 0.702	1.79×10^5	40.79	122.3	8.75×10^4
C4	0.948, 0.794	3.23×10^5	46.05	112.8	1.03×10^5
C5	0.958, 0.124	2.56×10^5	7.10	1524.2	2.87×10^6
C6	0.951, 0.233	1.58×10^5	13.47	492.5	6.20×10^5
C7	0.949, 0.342	1.47×10^5	19.86	306.8	3.38×10^5
C8	0.967, 0.087	4.49×10^5	4.99	3406.1	1.35×10^7
C9	0.958, 0.123	1.54×10^5	7.09	891.2	1.39×10^6

Table 6: Mass spectrum of particles and superparticles in the high-scale general gauge mediation.

Particle Masses (TeV)				
Pts	$m_{\tilde{g}}$	$m_{\tilde{t}_{1,2}}$	$m_{\tilde{b}_{1,2}}$	$m_{\tilde{\tau}_{1,2}}$
C1	1.80	1.17, 4.37	3.33, 4.37	1.18, 3.68
C2	1.27	0.61, 3.07	2.15, 3.06	0.68, 2.67
C3	1.63	0.68, 3.82	2.08, 3.81	0.89, 3.43
C4	2.84	1.54, 6.61	3.14, 6.61	2.08, 5.95
C5	2.29	1.48, 5.62	4.37, 5.61	1.59, 4.71
C6	1.46	0.52, 3.65	2.64, 3.65	1.00, 3.19
C7	1.36	0.31, 3.41	2.36, 3.40	0.84, 3.02
C8	3.90	2.07, 9.98	7.71, 9.98	2.89, 8.48
C9	1.43	0.71, 3.76	2.64, 3.76	1.14, 3.40

Particle Masses (GeV)				
Pts	$m_{\chi_1^c}$	$m_{\chi_1^0}$	$m_{h_{1,2,3}}$	$m_{a_{1,2}}$
C1	791.3	768.6	120.7, 777.4, 3665.7	194.8, 3665.7
C2	284.6	280.6	122.2, 559.6, 2443.0	139.6, 2442.9
C3	122.1	119.9	126.8, 639.4, 2207.5	155.3, 2207.4
C4	112.7	111.6	134.2, 878.8, 2792.8	211.2, 2792.7
C5	1522.3	1101.0	116.6, 1972.0, 4872.1	698.9, 4871.9
C6	491.3	486.7	121.2, 1274.9, 3068.7	446.3, 3068.4
C7	306.0	303.1	120.4, 1086.4, 2765.9	376.0, 2765.6
C8	3404.4	1981.1	120.1, 5084.2, 8909.4	2193.7, 8909.2
C9	889.0	771.4	117.2, 1884.6, 3306.1	806.7, 3305.3

Table 7: Composition of light Higgs bosons ($\leq 115\text{GeV}$). Here “Re” and “Im” denote the real and imaginary components of the neutral Higgs fields, respectively. All light Higgs bosons appearing in this paper are CP -odd, related to the explicitly breaking of the global $U(1)_R$ symmetry. However, all of them can satisfy the current experimental bounds since they are extremely singlet-like.

Composition of Light Higgs Bosons (LHB)				
Pts	LHBs	$\text{Im}(H_d)$	$\text{Im}(H_u)$	$\text{Im}(N)$
A1	a_1	-1.2×10^{-3}	-8.8×10^{-4}	0.999999
A2	a_1	-2.0×10^{-3}	-1.1×10^{-5}	0.999998
A3	a_1	-2.2×10^{-3}	9.4×10^{-4}	0.999997
A4	a_1	-2.1×10^{-3}	-7.5×10^{-5}	0.999998
A5	a_1	-2.0×10^{-4}	3.3×10^{-5}	> 0.9999995
A6	a_1	1.3×10^{-4}	-1.7×10^{-6}	> 0.9999995
A7	a_1	1.1×10^{-4}	6.1×10^{-5}	> 0.9999995
A9	a_1	4.6×10^{-3}	1.2×10^{-4}	0.999989
B1	a_1	-7.0×10^{-5}	-1.0×10^{-5}	> 0.9999995
B2	a_1	3.8×10^{-4}	1.7×10^{-5}	> 0.9999995

Table 8: Composition of the lightest neutralino or the NLSP in the low-scale general gauge mediation.

Composition of Lightest Neutralinos					
Pts	\tilde{B}	\tilde{W}^0	\tilde{H}_d	\tilde{H}_u	\tilde{N}
A1	0.021	-0.017	-0.451	-0.515	0.728
A2	-0.026	0.020	0.678	0.713	-0.173
A3	0.009	-0.006	0.710	-0.704	-0.024
A4	0.009	-0.006	0.710	-0.704	-0.019
A5	-0.020	0.017	0.658	0.687	-0.308
A6	-0.030	0.024	0.671	0.721	-0.172
A7	-0.027	0.020	0.679	0.722	-0.124
A8	-0.009	0.009	0.703	0.706	-0.083
A9	-0.026	0.022	0.686	0.711	-0.152

References

- [1] G. F. Giudice and A. Masiero, *Phys. Lett. B* **206**, 480 (1988).
- [2] T. S. Roy and M. Schmaltz, arXiv:0708.3593 [hep-ph]; H. Murayama, Y. Nomura and D. Poland, *Phys. Rev. D* **77**, 015005 (2008) [arXiv:0709.0775 [hep-ph]].
- [3] H. Y. Cho, arXiv:0802.1145 [hep-ph].
- [4] G. R. Dvali, G. F. Giudice and A. Pomarol, *Nucl. Phys. B* **478**, 31 (1996) [arXiv:hep-ph/9603238].
- [5] G. F. Giudice, H. D. Kim and R. Rattazzi, arXiv:0711.4448 [hep-ph].
- [6] M. Dine and A. E. Nelson, *Phys. Rev. D* **48**, 1277 (1993) [arXiv:hep-ph/9303230].
- [7] A. de Gouvea, A. Friedland and H. Murayama, *Phys. Rev. D* **57**, 5676 (1998) [arXiv:hep-ph/9711264].
- [8] G. F. Giudice and R. Rattazzi, *Nucl. Phys. B* **511**, 25 (1998) [arXiv:hep-ph/9706540].
- [9] T. Han, D. Marfatia and R. J. Zhang, *Phys. Rev. D* **61**, 013007 (2000) [arXiv:hep-ph/9906508].
- [10] A. Delgado, G. F. Giudice and P. Slavich, *Phys. Lett. B* **653**, 424 (2007) [arXiv:0706.3873 [hep-ph]].
- [11] P. Langacker, N. Polonsky and J. Wang, *Phys. Rev. D* **60**, 115005 (1999) [arXiv:hep-ph/9905252].
- [12] C. E. M. Wagner, *Nucl. Phys. B* **528**, 3 (1998) [arXiv:hep-ph/9801376].
- [13] M. Dine and J. D. Mason, arXiv:0712.1355 [hep-ph].
- [14] K. Jedamzik, M. Lemoine and G. Moultaqa, *Phys. Rev. D* **73**, 043514 (2006) [arXiv:hep-ph/0506129]; G. Moultaqa, *Acta Phys. Polon. B* **38**, 645 (2007) [arXiv:hep-ph/0612331].
- [15] LEP2 SUSY Working Group Combined LEP Chargino Results, up to 208 GeV.
[http://lepsusy.web.cern.ch/lepsusy/www/inos_moriond01/charginos_pub.html].
- [16] R. Barate *et al.* [LEP2 Higgs Working Group, ALEPH, DELPHI, L3 and OPAL Collaborations], *Phys. Lett. B* **565**, 61 (2003); LEP2 Higgs Working Group, ALEPH, DELPHI, L3 and OPAL experiments, note LHWG-Note-2004-01. [http://lephiggs.web.cern.ch/LEPHIGGS/papers/].

- [17] J. R. Espinosa and M. Quiros, Phys. Lett. B **266**, 389 (1991); M. S. Carena, J. R. Espinosa, M. Quiros and C. E. M. Wagner, Phys. Lett. B **355**, 209 (1995) [arXiv:hep-ph/9504316]; M. S. Carena, M. Quiros and C. E. M. Wagner, Nucl. Phys. B **461**, 407 (1996) [arXiv:hep-ph/9508343].
- [18] L. J. Hall, R. Rattazzi and U. Sarid, Phys. Rev. D **50**, 7048 (1994) [arXiv:hep-ph/9306309]; M. S. Carena, M. Olechowski, S. Pokorski and C. E. M. Wagner, Nucl. Phys. B **426**, 269 (1994) [arXiv:hep-ph/9402253].
- [19] B. A. Dobrescu and K. T. Matchev, JHEP **0009**, 031 (2000) [arXiv:hep-ph/0008192].
- [20] S. Ambrosanio, G. L. Kane, G. D. Kribs, S. P. Martin and S. Mrenna, Phys. Rev. D **54**, 5395 (1996) [arXiv:hep-ph/9605398].
- [21] R. L. Culbertson *et al.* [SUSY Working Group Collaboration], arXiv:hep-ph/0008070.
- [22] M. S. Carena, S. Pokorski and C. E. M. Wagner, Nucl. Phys. B **406**, 59 (1993) [arXiv:hep-ph/9303202]; P. Langacker and N. Polonsky, Phys. Rev. D **47**, 4028 (1993) [arXiv:hep-ph/9210235]; P. Langacker and N. Polonsky, Phys. Rev. D **52**, 3081 (1995) [arXiv:hep-ph/9503214].
- [23] A. Riotto and M. Trodden, Ann. Rev. Nucl. Part. Sci. **49**, 35 (1999) [arXiv:hep-ph/9901362].
- [24] P. Huet and A. E. Nelson, Phys. Rev. D **53**, 4578 (1996) [arXiv:hep-ph/9506477]; M. S. Carena, M. Quiros, A. Riotto, I. Vilja and C. E. M. Wagner, Nucl. Phys. B **503**, 387 (1997) [arXiv:hep-ph/9702409]; S. J. Huber and M. G. Schmidt, Nucl. Phys. B **606**, 183 (2001) [arXiv:hep-ph/0003122]; J. Kang, P. Langacker, T. j. Li and T. Liu, Phys. Rev. Lett. **94**, 061801 (2005) [arXiv:hep-ph/0402086]; A. Menon, D. E. Morrissey and C. E. M. Wagner, Phys. Rev. D **70**, 035005 (2004) [arXiv:hep-ph/0404184];
- [25] P. Nath, Phys. Rev. Lett. **66**, 2565 (1991); Y. Kizukuri and N. Oshimo, Phys. Rev. D **46**, 3025 (1992).
- [26] D. Suematsu, Eur. Phys. J. C **52**, 211 (2007) [arXiv:0706.3241 [hep-ph]].
- [27] S. F. King and P. L. White, Phys. Rev. D **52**, 4183 (1995) [arXiv:hep-ph/9505326].
- [28] S. Schael *et al.* [ALEPH Collaboration], Eur. Phys. J. C **47**, 547 (2006) [arXiv:hep-ex/0602042].
- [29] U. Ellwanger, J. F. Gunion, C. Hugonie and S. Moretti, arXiv:hep-ph/0305109; U. Ellwanger, J. F. Gunion and C. Hugonie, JHEP **0507**, 041 (2005) [arXiv:hep-ph/0503203]; S. Chang, P. J. Fox and N. Weiner, JHEP **0608**, 068 (2006) [arXiv:hep-ph/0511250]; U. Aglietti *et al.*, arXiv:hep-ph/0612172; K. Cheung, J. Song and Q. S. Yan, Phys. Rev. Lett. **99**, 031801 (2007) [arXiv:hep-ph/0703149]; S. Moretti, S. Munir and P. Poulose,

Phys. Lett. B **644**, 241 (2007) [arXiv:hep-ph/0608233]; P. W. Graham, A. Pierce and J. G. Wacker, arXiv:hep-ph/0605162; M. Carena, T. Han, G. Y. Huang and C. E. M. Wagner, arXiv:0712.2466 [hep-ph].

[30] J. Hisano, K. Kawagoe, R. Kitano and M. M. Nojiri, Phys. Rev. D **66**, 115004 (2002) [arXiv:hep-ph/0204078]; J. Hisano, K. Kawagoe and M. M. Nojiri, Phys. Rev. D **68**, 035007 (2003) [arXiv:hep-ph/0304214].

[31] Y. Santoso, arXiv:0709.3952 [hep-ph].

[32] M. Toharia and J. D. Wells, JHEP **0602**, 015 (2006) [arXiv:hep-ph/0503175].